



Parametric Analysis of a Universal Isotherm Model to Tailor Characteristics of Solid Desiccants for Dehumidification

Muhammad Burhan^{1*}, Qian Chen¹, Muhammad Wakil Shahzad², M Kum Ja¹ and Kim Choon Ng¹

¹Water Desalination and Reuse Centre (WDRC), Biological and Environmental Science & Engineering, King Abdullah University of Science and Technology (KAUST), Thuwal, Saudi Arabia, ²Northumbria University, Newcastle Upon Tyne, United Kingdom

OPEN ACCESS

Edited by:

Angelo Maiorino,
University of Salerno, Italy

Reviewed by:

Jani Dilip Batukray,
Government College of Engineering,
India
Andrea Frazzica,
Istituto di Tecnologie Avanzate per
l'Energia "Nicola Giordano" (ITAE), Italy

*Correspondence:

Muhammad Burhan
muhammad.burhan@kaust.edu.sa

Specialty section:

This article was submitted to
Process and Energy Systems
Engineering,
a section of the journal
Frontiers in Energy Research

Received: 05 February 2022

Accepted: 16 May 2022

Published: 28 June 2022

Citation:

Burhan M, Chen Q, Shahzad MW,
Ja MK and Ng KC (2022) Parametric
Analysis of a Universal Isotherm Model
to Tailor Characteristics of Solid
Desiccants for Dehumidification.
Front. Energy Res. 10:869807.
doi: 10.3389/fenrg.2022.869807

Cooling has a significant share in energy consumption, especially in hot tropical regions. The conventional mechanical vapor compression (MVC) cycle, widely used for air-conditioning needs, has high energy consumption as air is cooled down to a dew point to remove the moisture. Decoupling the latent cooling load through dehumidification from the sensible cooling load can significantly improve the energy requirement for air-conditioning applications. Solid desiccants have shown safe and reliable operation against liquid desiccants, and several configurations of solid desiccants dehumidifiers are studied to improve their performance. However, the characteristics of solid desiccants are critical for the performance and overall operation of the dehumidifier. The properties of every desiccant depend upon its porous adsorbing surface characteristics. Hence, it has an optimum performance for certain humid conditions. Therefore, for a better dehumidification performance in a specific tropical region, the solid desiccant must have the best performance, according to the humidity range of that region. In this article, a theoretical methodology has been discussed to help the industry and chemists to understand the porous structural properties of adsorbent surfaces needed to tune the material performance for a particular humidity value before material synthesis.

Keywords: dehumidification, adsorbent, material, isotherm, cooling

1 INTRODUCTION

Under climate change and weather intensity, air conditioning is becoming inevitable for the comfort of human beings. Air conditioning demand is very high in hot and humid tropical regions with high humidity (Samuel et al., 2013; Fekadu and Subudhi, 2018; Burhan et al., 2021a). Such a humid tropical climate demands a higher latent than sensible cooling load. The mechanical vapor compression (MVC) cycle is widely and conventionally employed across the globe to fulfill such cooling needs. The MVC has to cool down the air at a very low temperature of a dew point level, way below the comfort level needs. This leads to the waste of high-grade electrical energy (Barbosa et al., 2012; Park et al., 2015; Oh et al., 2019). On the other hand, the utilization of CFC refrigerants is harmful to the environment and human beings (Chen et al., 2021c; Rabah Touaibi and Hasan Koten, 2021).

To minimize the high energy consumption of the cooling needs, one possible solution is decoupling the air conditioning systems' latent and sensible cooling loads. Desiccant dehumidifiers provide one of the solutions to decouple the latent load from the total cooling

load (Oh et al., 2017; Chen et al., 2020a; El Loubani et al., 2021). Furthermore, solid desiccants are proven reliable and compact compared to liquid desiccants, which pose several health risks. They were found to have carryover and are toxic and corrosive (Liu et al., 2019; Gurubalan and Simonson, 2021). In the humid tropical climate, therefore, the air conditioner's performance relies on the performance of the desiccant dehumidification system. The dehumidification system efficiency depends upon two main factors: the properties and performance of the desiccant material and the design of the desiccant system for better heat and mass transfer. Recently, many efforts have been made on the design of desiccant dehumidification systems like rotary wheels and coated heat exchangers (Zhou and Reece, 2019; Venegas et al., 2021). However, the characteristics of the desiccant material are critical (Muthu et al., 2021) to enhance the performance as different characteristics of the desiccant are needed for other tropical locations depending upon the humidity level for the optimum performance of the desiccant.

Understanding the adsorption phenomena is very important for many industrial applications (Kawamoto et al., 2016; Burhan et al., 2019a; Chorowski et al., 2019; Chen et al., 2020b; Zakuciová et al., 2020; Chen et al., 2021a; Chen et al., 2021b; Ja et al., 2022), and each adsorbent adsorbate pair has unique characteristics (Kresge et al., 1992; Zhao et al., 1998; Chen et al., 2020c; Chen et al., 2021c). Due to these unique characteristics, six different adsorption isotherms depend upon their shape, as defined by the International Union of Pure and Applied Chemistry (IUPAC) (Chakraborty and Sun, 2014; Ng et al., 2017). Each adsorbent pair has different uptake levels at different pressure levels, either single or double layers. This behavior depends upon the surface topography of the adsorbent and the energy level heterogeneity of the available adsorption sites (Burhan et al., 2021b).

In desiccant dehumidification, the space humidity needs to match with the operating range of the adsorbent. Some adsorbents reach their saturation limit at a very low partial pressure or humidity level. Such desiccant materials cannot be suitable for dehumidification as they will always be saturated even in normal conditions as space humidity does not go to such a low level. On the other hand, adsorbents with saturation limits at higher humidity levels may or may not be suitable for desiccant dehumidification, depending on their characteristics or isotherms. The important factors are the point of partial pressure when the uptake starts and when it reaches its saturation limit, the slope of such a rise in uptake, and the difference between these two points. Ideally, for dehumidification purposes, the starting point of the uptake must be according to the humidity level of the space. The saturation point must also be the same as the starting point, making a difference and slope theoretically as zero and infinity, respectively. This is not possible in practical, but efforts are made during material synthesis to get closer to such performance.

Chemists adopt many recipes to tailor the performance of the adsorbents during material synthesis (Burhan et al., 2019b). However, the post-processing analysis after material synthesis defines whether the required characteristics have been successfully achieved or not and to what extent the ideal limit

is. The objective of this manuscript was to theoretically demonstrate how adsorbent surface topography should be altered during material synthesis to tailor the required response of the material, especially focusing on the desiccant dehumidification point of view. This manuscript will explain how desiccant topography can be altered to enhance and tailor its response for the dehumidification application and how adsorbent surface parameters will be changed to achieve such a response. This methodology will provide information about the required change in the surface parameters before material synthesis to get the desired properties for the optimized dehumidification need.

2 METHODOLOGY

To understand the unique interaction of the adsorbent adsorbate pair and the adsorption phenomena, a universal isotherm model was developed based upon the classic adsorption theory. The universal isotherm model follows all six isotherm types and describes the formation of these isotherm shapes. The main advantage of the universal isotherm model is that it clearly shows the characteristics of the adsorption surface for each isotherm type in the form of the distribution of adsorption energy sites and their availability. The adsorption surface is made of tiny pores or adsorption sites having different energy levels. When the adsorbate reaches a certain critical energy level, i.e., $\epsilon_c = -RT \ln Kp$, it is adsorbed in the adsorption site with an energy level corresponding to the critical energy level of the adsorbate. When the partial pressure of the adsorbate changes, its critical energy level also changes. As a result, the availability of adsorption energy sites for adsorption also changes. However, depending upon the quantity of such availability describes the total uptake at that partial pressure, i.e.,

$$\theta_t = \int_{\epsilon_c}^{\infty} X(\epsilon) d\epsilon. \quad (1)$$

Figure 1: shows the characteristics of the adsorption isotherm and its association with the porous adsorbent surface and energy distribution of energy of these adsorption sites. Many factors affect the characteristics of the adsorption isotherm, like its rate of total adsorption uptake over a range of partial pressures, the starting point of the adsorption uptake, the saturation point of the total adsorption uptake, and the total uptake of the adsorbent. To understand the link between these factors on the adsorption isotherms, the universal isotherm model has provided the energy distribution function (EDF) for the adsorption energy sites as

$$X(\epsilon) = \sum_{i=1}^n \alpha_i \left\{ \frac{\exp\left(\frac{\Delta\epsilon - \epsilon_{oi}}{m_i}\right)}{m_i \left[1 + \exp\left(\frac{\Delta\epsilon - \epsilon_{oi}}{m_i}\right)\right]^2} \right\}_i. \quad (2)$$

For the two isotherms, brown and blue, the corresponding energy distribution function (EDF) curves are shown in the exact figure at the bottom right corner in **Figure 1**. The color of the EDF curves corresponds to the same color isotherms.

The universal isotherm model successfully defined all isotherm types and understood the formation of such shapes.

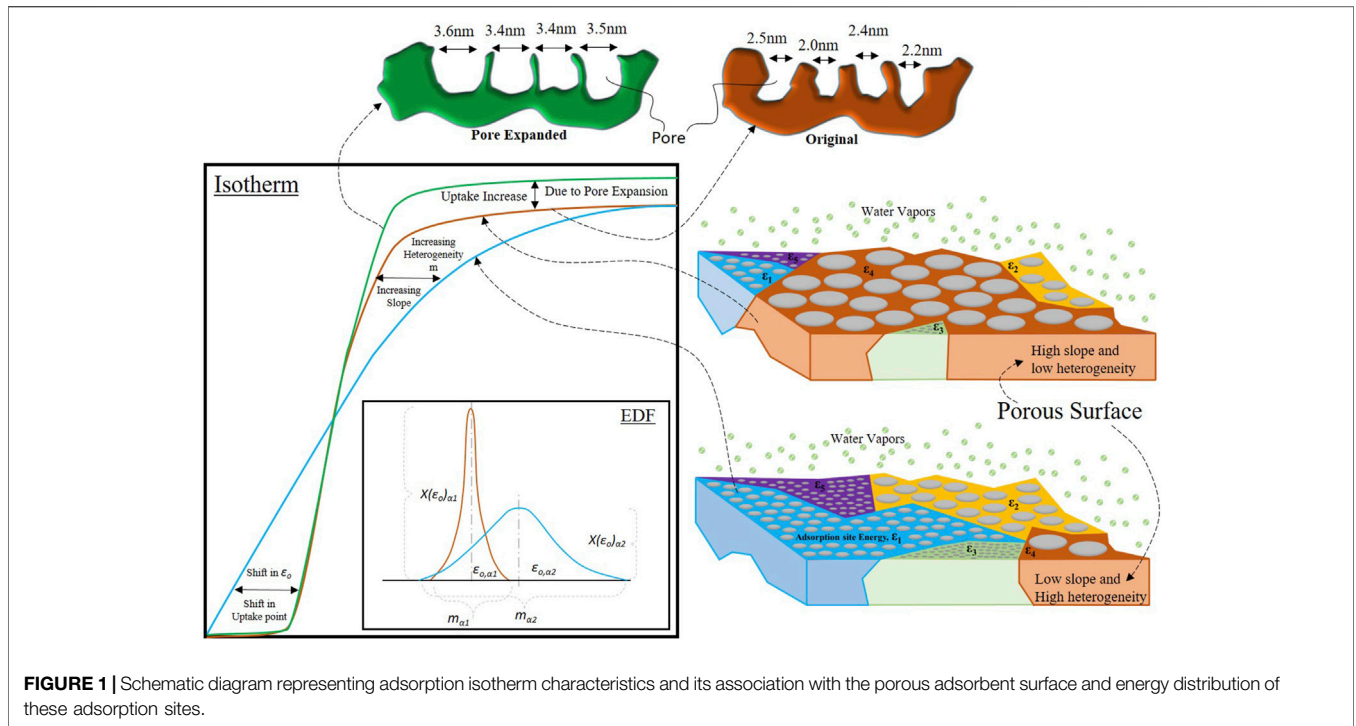


FIGURE 1 | Schematic diagram representing adsorption isotherm characteristics and its association with the porous adsorbent surface and energy distribution of these adsorption sites.

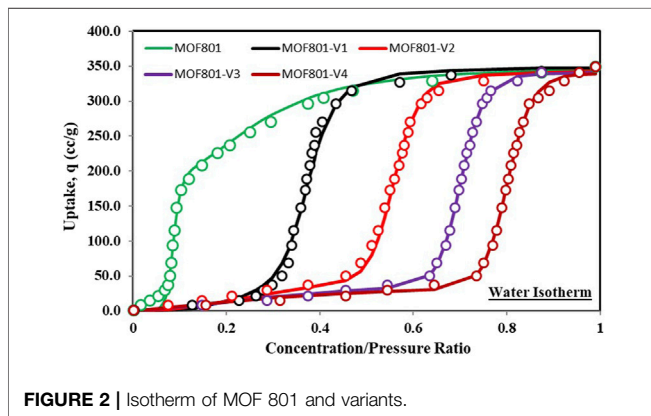


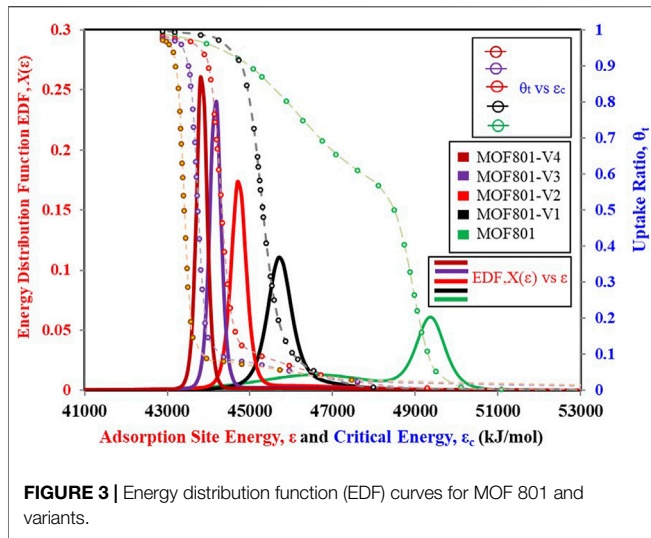
FIGURE 2 | Isotherm of MOF 801 and variants.

However, the primary importance of understanding the adsorption phenomena is in material synthesis so that the performance of the material can be tuned as per application. The material scientists can modify its performance by changing its porous surface characteristics or distribution of the adsorption energy sites and their availability. Such changes can be adopted during material synthesis by the pore expansion and surface treatment techniques like heat treatment (Young, 1958; Baker and Sing, 1976; Naono et al., 1980; Shioji et al., 2001; Alrowais et al., 2020; Chen et al., 2021d), chemical action (Ishikawa et al., 1996; Burhan, 2015), and acidification (Toor and Jin, 2012). These changes are directly linked to the parameters associated with the EDF equation of the universal isotherm model.

As described earlier, certain factors define the characteristics of the adsorption isotherm, and out of them, the total uptake of

the adsorbent material is not linked with the EDF. The increase in the total uptake, as shown in **Figure 2**, depends on the increased capacity of the adsorbent material. This material capacity can be increased by pore expansion or increased pore volume or surface area. However, the rest of the characteristics, like change in the rate of total uptake and the point of uptake, depend upon the distribution of the adsorption energy site. Adsorption surface heterogeneity ‘*m*’, the energy level of the median adsorption site ‘ ϵ_o ’, and its fractional availability ‘*X*(ϵ)’ are the main parameters in the EDF equation defining the shape of the isotherm. By controlling these parameters through pore expansion, the isotherms of the adsorbent can be tuned as per the certain requirement of the application. As the pore size and distribution are associated with the energy of the adsorption site, therefore, by adopting the pore expansion techniques of heat treatment [Young, (1958); Baker and Sing, (1976); Naono et al., (1980); Shioji et al., (2001); Alrowais et al., (2020); Chen et al., (2021d)], chemical action (Ishikawa et al., 1996; Burhan, 2015), and acidification (Toor and Jin, 2012), the pore distribution and, as a result, the energy distribution of the material can be tailored for the required isotherms. **Figure 1** demonstrates how a change in the isotherm is associated with the EDF curve and how the porous structure of the adsorbent surface changes.

The blue isotherm line represents a typical isotherm curve, and the corresponding EDF curve is also shown in **Figure 1**. The spread or width of the EDF curves is based upon the value of the surface heterogeneity ‘*m*’. The curve’s middle point defines the median energy level ‘ ϵ_o ’, and the curve’s height at the median energy level defines its fractional availability ‘*X*(ϵ)’ against the other available adsorption energy sites. The porous surface of the adsorbent is represented by the illustration at the bottom right



corner of **Figure 1**. However, with the pore expansion and material synthesis, the porous structure of the adsorbent surface is turned into the illustration at the top right corner of **Figure 1**. It can be seen that with the pore expansion, the smaller pores with energy levels ϵ_1 , ϵ_2 , and ϵ_3 are expanded to the bigger pores of the energy level ϵ_4 . As a result, the availability of adsorption sites with energy level ϵ_4 is higher, which can be seen from the brown EDF curve as the median energy level is shifted toward the left, and its fractional availability 'X(ϵ)' is high as compared to the blue EDF curve. On the other hand, the brown EDF curve's heterogeneity 'm' or width is reduced. This is because most of the small pores are now expanded to bigger pores and no longer exist. This is why the EDF is taller, and the slope of the brown isotherm increases, resulting in a higher rate of adsorption uptake. Because once the critical energy level reaches the energy level of the pores with the higher fractional availability, there is a sudden uptake increase as compared to the blue isotherm, in which the uptake is gradual as per the gradual availability of the adsorption sites due to high heterogeneity. The uptake point of the brown isotherm curve is also shifted toward the higher partial pressure side due to a shift in the median energy level toward the left or lower energy value side.

3 RESULTS AND DISCUSSION

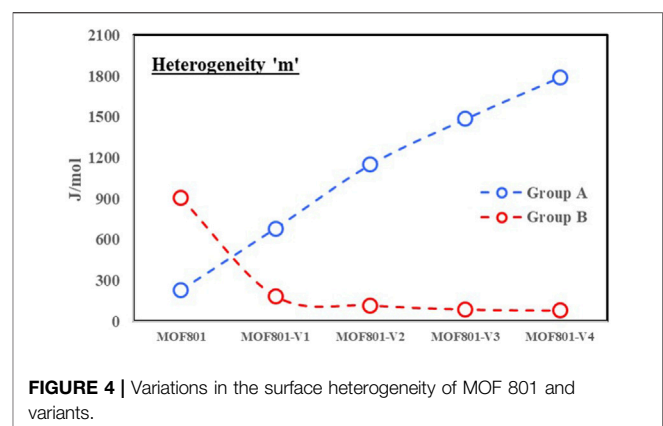
As per the explanation provided in the methodology, in this section, the performance of the adsorbents will be tuned according to the dehumidification point of view. It will be analyzed how the surface characteristics of the adsorbent material are modified to achieve the required isotherm of the material for better performance. From a dehumidification point of view, the best materials are the S-shape isotherms. Therefore, the materials with the S-shape isotherms will only be analyzed.

Figure 2 shows the isotherm of MOF 801 (Furukawa et al., 2014) in the green line. However, the uptake starting point is at a very low concentration ratio of humidity levels. This adsorbent is

unsuitable for dehumidification in humidity regions because it requires very dry conditions to regenerate. To make it ideal for dehumidification for areas with different humidity levels, the uptake starting point must be shifted toward higher concentration ratios, as depicted by black, red, purple, and brown lines in **Figure 2**. Their corresponding EDF curves are also shown in **Figure 3**. From the EDF curves, it can be seen that as the uptake point of the adsorption isotherm is shifting toward a higher pressure ratio, the EDF curve i.e., ' ϵ_0 ' is shifting toward the left, i.e., the lower energy level. It depicts that a higher concentration/pressure ratio must be achieved for pores with very low energy levels. It can also be seen that the width of EDF or heterogeneity 'm' of the porous adsorbent surface is decreasing and the fractional availability 'X(ϵ)' of the median energy site ' ϵ_0 ' is increasing. This is why the EDF curves and the corresponding isotherm curve are getting steep. Therefore, the uptake starting point of the isotherm can be shifted to the high-pressure ratio or the humidity level if the median energy level of the adsorption energy sites is shifted toward the lower value. The shift in the energy level must be according to the required humidity in which the adsorbent will be employed.

Moreover, in these isotherms, the main focus is to shift the pressure ratio of the isotherms only. This is why the pore expansion is only shifting the median energy level. However, the total uptake has been kept the same because the increase in total uptake with the pore expansion also requires structural stability and additional parameters and testing to make it feasible for the industrial application. But, here, the pore expansion also increases the surface heterogeneity of the adsorbent and the fractional availability of energy sites. Therefore, the slope or the rate of total uptake grows toward a high-pressure ratio.

A universal isotherm model with two terms was used to fit all of the isotherms shown in **Figure 2**, and from that, the obtained value of the surface heterogeneity is shown in **Figure 4**. As it was based on two terms, two heterogeneity values are shown because the material has two groups of the adsorption sites, and the share of each adsorption site's groups in these isotherms and the EDF curve is shown in **Figure 5**. For the first isotherm, the percentage of each group of adsorption sites is almost the same. This is why in **Figure 3**, we can see two green EDF curves, and their heterogeneity values are shown in **Figure 4**, where the red line



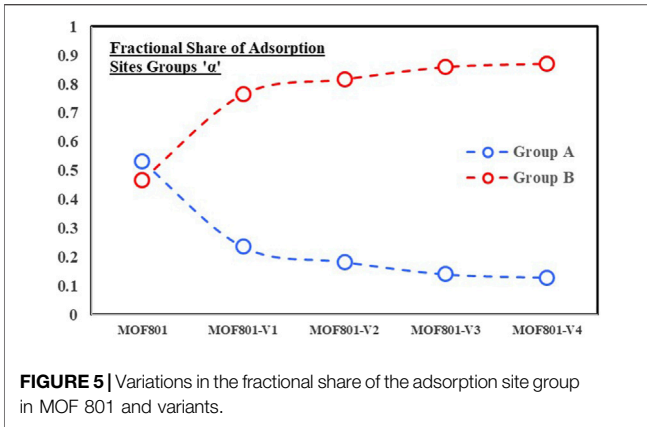


FIGURE 5 | Variations in the fractional share of the adsorption site group in MOF 801 and variants.

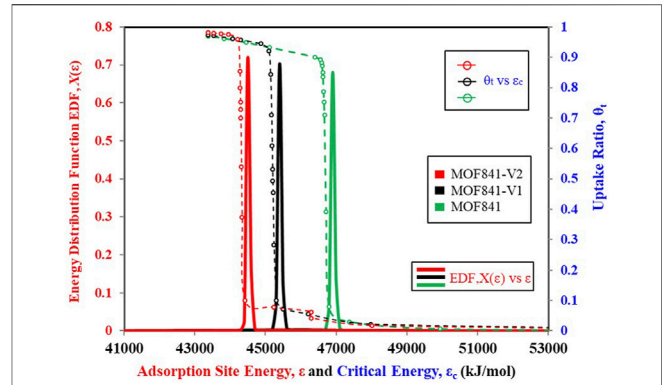


FIGURE 7 | Energy distribution function (EDF) curves for MOF 801 and variants.

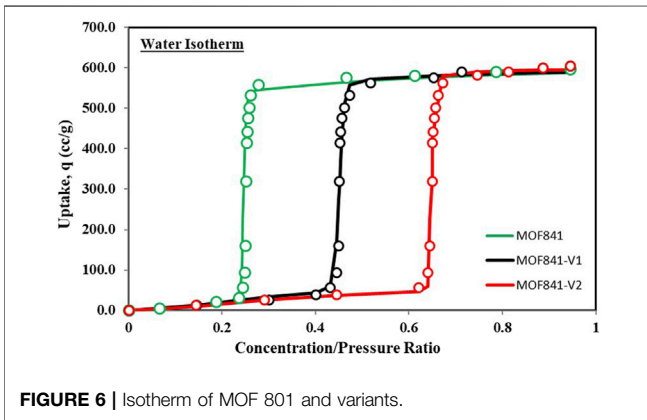


FIGURE 6 | Isotherm of MOF 801 and variants.

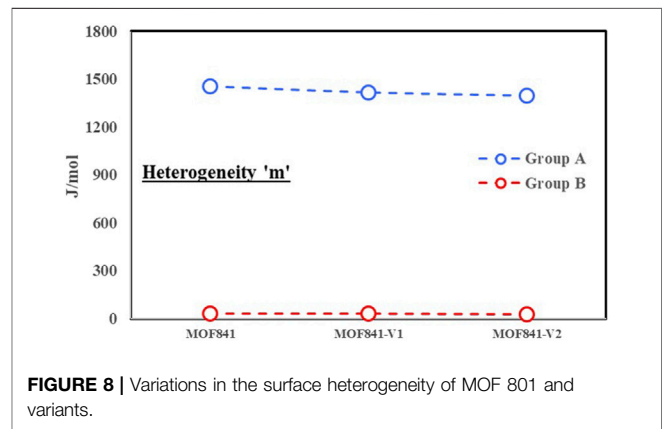


FIGURE 8 | Variations in the surface heterogeneity of MOF 801 and variants.

is associated with the EDF curves with the highest 'X(ε)' values, except for the first isotherm. The heterogeneity of the first isotherm is less for the first group of the adsorption site, causing a sharp rise or a higher slope at the initial value of the pressure. However, at higher pressure ratios, the effect of the second group of adsorption sites comes into effect. The heterogeneity increases, causing a gradual increase in the total uptake and a decrease in the slope. For the other four isotherms, only one group of the adsorption sites has a dominant effect which can be seen from the gap of both curves in **Figure 5**. This is why only one EDF curve is visible in **Figure 3** for these results, for which the heterogeneity value is very low and almost constant, the red curve in **Figure 4**, causing a steep rise in the total uptake. The blue line shows high heterogeneity, representing the part of the isotherm before a sudden rise in the total uptake.

In the previous isotherm result, with the shift in the uptake point, the heterogeneity of the porous surface also changed. **Figure 6** shows the MOF 841 isotherm (green line) (Furukawa et al., 2014), an ideal S-shape for the dehumidification application but operating in the low-pressure ratio range or the humidity region. Therefore, the need is to shift the uptake point to the high-pressure ratio without affecting the original high rate of the uptake, i.e., the heterogeneity of the porous surface. The other two isotherms (black and red lines) with the uptake at high-pressure ratio points are shown in **Figure 6**, and the

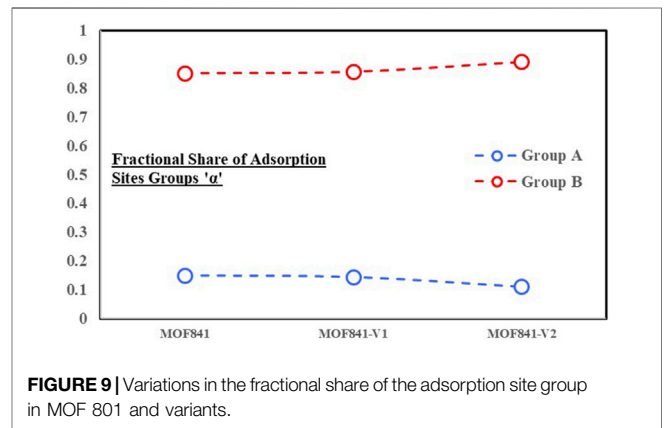


FIGURE 9 | Variations in the fractional share of the adsorption site group in MOF 801 and variants.

corresponding EDF curves are demonstrated in **Figure 7**. From the EDF curves in **Figure 7**, it can be seen that the width or heterogeneity 'm' of all of the EDF curves is the same along with the fractional availability 'X(ε)' of the median energy level. This is why all of the isotherms depict a similar rate of the total uptake or slope of the isotherm. As the median energy level 'ε₀' shifts toward a lower energy level, the pressure ratio for adsorption uptake shifts to a higher value.

Similar to the previous results, the two terms of the universal isotherm model were used to fit these three isotherms, and the obtained value of their heterogeneity 'm' and the probability share of each adsorption sites group are shown in **Figures 8, 9**. From **Figure 8**, it can be seen that the heterogeneity value is the same for all the three isotherms. In addition, its value is very low for the red line as it represents the group of the adsorption sites group with a share of more than 85%. Although other groups have higher and similar heterogeneity, due to their low share of less than 15%, they are not significantly contributing to the EDF curve, which is why such a large deviation of results between groups A and B can be seen in **Figures 8, 9**.

These results show that by changing the structural parameters, one can achieve the desired structural characteristics of a porous adsorbent surface. As a result, it can tune the adsorbent's performance for the optimized application. This tool and methodology have significance in the dehumidification industry as the humid conditions vary from region to region. Although the examples of MOF materials are considered and analyzed in this manuscript, the methodology applies to all adsorbents with physical adsorption. A case of silica is already discussed in our previous publication (Burhan et al., 2019b). This also proves the validation of the methodology and the results. Therefore, with the help of this tool, the industry can understand the porous structural properties of the adsorbent surface needed to tune the material performance for a particular humidity value. Thus, by following the results of this methodology, the material can be synthesized and optimized for a specific humidity with significant energy savings.

REFERENCES

- Alrowais, R., Qian, C., Burhan, M., Ybyraiyimkul, D., Shahzad, M. W., and Ng, K. C. (2020). A Greener Seawater Desalination Method by Direct-Contact Spray Evaporation and Condensation (DCSEC): Experiments. *Appl. Therm. Eng.* 179, 115629. doi:10.1016/j.applthermaleng.2020.115629
- Baker, F. S., and Sing, K. S. W. (1976). Specificity in the Adsorption of Nitrogen and Water on Hydroxylated and Dehydroxylated Silicas. *J. Colloid Interface Sci.* 55 (3), 605–613. doi:10.1016/0021-9797(76)90071-0
- Barbosa, J. R., Jr, Ribeiro, G. B., and de Oliveira, P. A. (2012). A State-Of-The-Art Review of Compact Vapor Compression Refrigeration Systems and Their Applications. *Heat. Transf. Eng.* 33 (4-5), 356–374. doi:10.1080/01457632.2012.613275
- Burhan, M., Akhtar, F. H., Chen, Q., Shahzad, M. W., Ybyraiyimkul, D., and Ng, K. C. (2021). A Universal Mathematical Methodology in Characterization of Materials for Tailored Design of Porous Surfaces. *Front. Chem.* 8, 1237. doi:10.3389/fchem.2020.601132
- Burhan, M., Shahzad, M. W., and Ng, K. C. (2019). A Universal Theoretical Framework in Material Characterization for Tailored Porous Surface Design. *Sci. Rep.* 9 (1), 8773–8777. doi:10.1038/s41598-019-45350-5
- Burhan, M. (2015). *Theoretical and Experimental Study of Concentrated Photovoltaic (CPV) System with Hydrogen Production as Energy Storage*. Singapore: Scholar Bank NUS.
- Burhan, M., Chen, Q., Shahzad, M. W., Ybyraiyimkul, D., Akhtar, F. H., and Ng, K. C. (2021). Innovative Concentrated Photovoltaic Thermal (CPV/T) System with Combined Hydrogen and MgO Based Storage. *Int. J. Hydrogen Energy* 46 (31), 16534–16545. doi:10.1016/j.ijhydene.2020.09.163

4 CONCLUSION

A theoretical methodology has been presented to understand the adsorbent performance by modifying the surface parameters. The proposed methodology can help the industry and chemists to tune and optimize the material performance for the dehumidification of air, especially in the desired humidity range. The required porous structure in terms of surface heterogeneity, distribution of adsorption energy sites, and the fraction of availability of each adsorption site can be predicted. For dehumidification, the desiccant should have a lower heterogeneity level and a higher fractional availability, i.e., >85% for the higher rate of the adsorption uptake. At the concentration ratio where a high adsorption uptake is required, the adsorption energy site ϵ_0 equivalent to the critical energy level ϵ_c of that pressure ratio point must be in a high fractional availability $X(\epsilon)$, i.e., >85%. Thus, the adsorbent can be synthesized accordingly to have the tuned isotherm for optimized performance by knowing the required distribution of adsorption energy sites.

DATA AVAILABILITY STATEMENT

The raw data supporting the conclusions of this article will be made available by the authors, without undue reservation.

AUTHOR CONTRIBUTIONS

MB wrote the manuscript. MB, QC, MKJ, and KN discussed and analyzed the results and reviewed the manuscript.

- Burhan, M., Shahzad, M. W., Ybyraiyimkul, D., Oh, S. J., Ghaffour, N., and Ng, K. C. (2019). Performance Investigation of MEMSYS Vacuum Membrane Distillation System in Single Effect and Multi-Effect Mode. *Sustain. Energy Technol. Assessments* 34, 9–15. doi:10.1016/j.seta.2019.04.003
- Chakraborty, A., and Sun, B. (2014). An Adsorption Isotherm Equation for Multi-Types Adsorption with Thermodynamic Correctness. *Appl. Therm. Eng.* 72 (2), 190–199. doi:10.1016/j.applthermaleng.2014.04.024
- Chen, Q., Burhan, M., Kum Ja, M., Li, Y., and Choon Ng, K. (2021). A Spray-Assisted Multi-Effect Distillation System Driven by Ocean Thermocline Energy. *Energy Convers. Manag.* 245, 114570. doi:10.1016/j.enconman.2021.114570
- Chen, Q., Burhan, M., M., K. J., Li, Y., and Ng, K. C. (2021). An Ocean Thermocline Desalination System Using the Direct Spray Method. *Desalination* 520, 115373. doi:10.1016/j.desal.2021.115373
- Chen, Q., Burhan, M., and Oh, S. J. (2021). A Brief Review of Solar Indoor Lighting System Integrated with Optofluidic Technologies. *Energy Tech.* 9 (5), 2001099. doi:10.1002/ente.202001099
- Chen, Q., Burhan, M., Shahzad, M. W., Ybyraiyimkul, D., Akhtar, F. H., and Ng, K. C. (2020). Simultaneous Production of Cooling and Freshwater by an Integrated Indirect Evaporative Cooling and Humidification-Dehumidification Desalination Cycle. *Energy Convers. Manag.* 221, 113169. doi:10.1016/j.enconman.2020.113169
- Chen, Q., Kum Ja, M., Burhan, M., Akhtar, F. H., Shahzad, M. W., Ybyraiyimkul, D., et al. (2021). A Hybrid Indirect Evaporative Cooling-Mechanical Vapor Compression Process for Energy-Efficient Air Conditioning. *Energy Convers. Manag.* 248, 114798. doi:10.1016/j.enconman.2021.114798
- Chen, Q., Muhammad, B., Akhtar, F. H., Ybyraiyimkul, D., Muhammad, W. S., Li, Y., et al. (2020). Thermo-economic Analysis and Optimization of a Vacuum Multi-Effect Membrane Distillation System. *Desalination* 483, 114413. doi:10.1016/j.desal.2020.114413

- Chen, Q., Oh, S. J., and Burhan, M. (2020). Design and Optimization of a Novel Electrowetting-Driven Solar-Indoor Lighting System. *Appl. Energy* 269, 115128. doi:10.1016/j.apenergy.2020.115128
- Chorowski, M., Pyrka, P., Rogala, Z., and Czupryński, P. (2019). Experimental Study of Performance Improvement of 3-Bed and 2-Evaporator Adsorption Chiller by Control Optimization. *Energies* 12 (20), 3943. doi:10.3390/en12203943
- El Loubani, M., Ghaddar, N., Ghali, K., and Itani, M. (2021). Hybrid Cooling System Integrating PCM-Desiccant Dehumidification and Personal Evaporative Cooling for Hot and Humid Climates. *J. Build. Eng.* 33, 101580. doi:10.1016/j.jobe.2020.101580
- Fekadu, G., and Subudhi, S. (2018). Renewable Energy for Liquid Desiccants Air Conditioning System: A Review. *Renew. Sustain. Energy Rev.* 93, 364–379. doi:10.1016/j.rser.2018.05.016
- Furukawa, H., Gándara, F., Zhang, Y.-B., Jiang, J., Queen, W. L., Hudson, M. R., et al. (2014). Water Adsorption in Porous Metal-Organic Frameworks and Related Materials. *J. Am. Chem. Soc.* 136 (11), 4369–4381. doi:10.1021/ja500330a
- Gurubalan, A., and Simonson, C. J. (2021). A Comprehensive Review of Dehumidifiers and Regenerators for Liquid Desiccant Air Conditioning System. *Energy Convers. Manag.* 240, 114234. doi:10.1016/j.enconman.2021.114234
- Ishikawa, T., Matsuda, M., Yasukawa, A., Kandori, K., Inagaki, S., Fukushima, T., et al. (1996). Surface Silanol Groups of Mesoporous Silica FSM-16. *Faraday Trans.* 92 (11), 1985–1989. doi:10.1039/ft9969201985
- Ja, M. K., Chen, Q., Burhan, M., Ybyraiymkul, D., Shahzad, M. W., Alrowais, R., et al. (2022). Direct Contact Heat and Mass Exchanger for Heating, Cooling, Humidification, and Dehumidification. *Heat. Exch.*, 95. doi:10.5772/intechopen.102353
- Kawamoto, K., Cho, W., Kohno, H., Koganei, M., Ooka, R., and Kato, S. (2016). Field Study on Humidification Performance of a Desiccant Air-Conditioning System Combined with a Heat Pump. *Energies* 9 (2), 89. doi:10.3390/en9020089
- Kresge, C. T., Leonowicz, M. E., Roth, W. J., Vartuli, J. C., and Beck, J. S. (1992). Ordered Mesoporous Molecular Sieves Synthesized by a Liquid-Crystal Template Mechanism. *nature* 359 (6397), 710–712. doi:10.1038/359710a0
- Liu, X., Qu, M., Liu, X., and Wang, L. (2019). Membrane-based Liquid Desiccant Air Dehumidification: A Comprehensive Review on Materials, Components, Systems and Performances. *Renew. Sustain. Energy Rev.* 110, 444–466. doi:10.1016/j.rser.2019.04.018
- Muthu, S., Sekarapandian, N., and Ashok, K. (2021). Performance Enhancement of Rotary Desiccant Wheel Using Novel Homogenous Composite Desiccant Designs IOP Conference Series: Materials Science and Engineering. *IOP Publ.* 1123 (No. 1), 012055. doi:10.1088/1757-899x/1123/1/012055
- Naono, H., Fujiwara, R., and Yagi, M. (1980). Determination of Physisorbed and Chemisorbed Waters on Silica Gel and Porous Silica Glass by Means of Desorption Isotherms of Water Vapor. *J. Colloid Interface Sci.* 76 (1), 74–82. doi:10.1016/0021-9797(80)90272-6
- Ng, K. C., Burhan, M., Shahzad, M. W., and Ismail, A. B. (2017). A Universal Isotherm Model to Capture Adsorption Uptake and Energy Distribution of Porous Heterogeneous Surface. *Sci. Rep.* 7 (1), 10634. doi:10.1038/s41598-017-11156-6
- Oh, S. J., Ng, K. C., Chun, W., and Chua, K. J. E. (2017). Evaluation of a Dehumidifier with Adsorbent Coated Heat Exchangers for Tropical Climate Operations. *Energy* 137, 441–448. doi:10.1016/j.energy.2017.02.169
- Oh, S. J., Shahzad, M. W., Burhan, M., Chun, W., Kian Jon, C., KumJa, M., et al. (2019). Approaches to Energy Efficiency in Air Conditioning: a Comparative Study on Purge Configurations for Indirect Evaporative Cooling. *Energy* 168, 505–515. doi:10.1016/j.energy.2018.11.077
- Park, C., Lee, H., Hwang, Y., and Radermacher, R. (2015). Recent Advances in Vapor Compression Cycle Technologies. *Int. J. Refrig.* 60, 118–134. doi:10.1016/j.ijrefrig.2015.08.005
- Rabah Touaibi, R., and Hasan Koten, H. (2021). Energy Analysis of Vapor Compression Refrigeration Cycle Using a New Generation Refrigerants with Low Global Warming Potential. *Arfms* 87 (2), 106–117. doi:10.37934/arfms.87.2.106117
- Samuel, D. G. L., Nagendra, S. M. S., and Maiya, M. P. (2013). Passive Alternatives to Mechanical Air Conditioning of Building: A Review. *Build. Environ.* 66, 54–64. doi:10.1016/j.buildenv.2013.04.016
- Shioji, S., Kawaguchi, M., Hayashi, Y., Tokami, K., and Yamamoto, H. (2001). Rehydroxylation of Dehydrated Silica Surfaces by Water Vapor Adsorption. *Adv. Powder Technol.* 12 (3), 331–342. doi:10.1163/156855201750537884
- Toor, M., and Jin, B. (2012). Adsorption Characteristics, Isotherm, Kinetics, and Diffusion of Modified Natural Bentonite for Removing Diazo Dye. *Chem. Eng. J.* 187, 79–88. doi:10.1016/j.ccej.2012.01.089
- Venegas, T., Qu, M., Nawaz, K., and Wang, L. (2021). Critical Review and Future Prospects for Desiccant Coated Heat Exchangers: Materials, Design, and Manufacturing. *Renew. Sustain. Energy Rev.* 151, 111531. doi:10.1016/j.rser.2021.111531
- Young, G. J. (1958). Interaction of Water Vapor with Silica Surfaces. *J. Colloid Sci.* 13 (1), 67–85. doi:10.1016/0095-8522(58)90010-2
- Zakuciová, K., Štefanica, J., Carvalho, A., and Kočí, V. (2020). Environmental Assessment of a Coal Power Plant with Carbon Dioxide Capture System Based on the Activated Carbon Adsorption Process: A Case Study of the Czech Republic. *Energies* 13 (9), 2251.
- Zhao, D., Feng, J., Huo, Q., Melosh, N., Fredrickson, G. H., Chmelka, B. F., et al. (1998). Triblock Copolymer Syntheses of Mesoporous Silica with Periodic 50 to 300 Ångstrom Pores. *science* 279 (5350), 548–552. doi:10.1126/science.279.5350.548
- Zhou, X., and Reece, R. (2019). Experimental Investigation for a Non-adiabatic Desiccant Wheel with a Concentric Structure at Low Regeneration Temperatures. *Energy Convers. Manag.* 201, 112165. doi:10.1016/j.enconman.2019.112165

Conflict of Interest: The authors declare that the research was conducted in the absence of any commercial or financial relationships that could be construed as a potential conflict of interest.

Publisher's Note: All claims expressed in this article are solely those of the authors and do not necessarily represent those of their affiliated organizations, or those of the publisher, the editors, and the reviewers. Any product that may be evaluated in this article, or claim that may be made by its manufacturer, is not guaranteed or endorsed by the publisher.

Copyright © 2022 Burhan, Chen, Shahzad, Ja and Ng. This is an open-access article distributed under the terms of the Creative Commons Attribution License (CC BY). The use, distribution or reproduction in other forums is permitted, provided the original author(s) and the copyright owner(s) are credited and that the original publication in this journal is cited, in accordance with accepted academic practice. No use, distribution or reproduction is permitted which does not comply with these terms.

NOMENCLATURE

ϵ adsorption site energy (kJ/mol)

$X(\epsilon)$ energy distribution function

ϵ_0 adsorption site energy with highest availability (kJ/mol)

K adsorption equilibrium constant

θ_t total adsorption uptake

m surface heterogeneity (J/mol)

ϵ_c critical energy level (kJ/mol)

R general gas constant (J/molK)

T adsorbent temperature (K)

p adsorbate pressure (Pa)

α probability of the adsorption site group